Permittivity Measurement of Liquids, Powders and Suspensions using a Parallel-Plate Cell

Atefeh Kordzadeh[1,2], Nicola De Zanche[3,4]

1. Department of Biomedical Engineering, University of Alberta, Edmonton, Alberta, Canada
2. Department of Electrical and Computer Engineering, University of Alberta, Edmonton, Alberta, Canada
3. Department of Medical Physics, Cross Cancer Institute, Edmonton, Alberta, Canada
4. Department of Oncology, University of Alberta, Edmonton, Alberta, Canada

Published in

Concepts in Magnetic Resonance part B: Magnetic Resonance Engineering

DOI: 10.1002/cmr.b.21318

***Corresponding author:**

Nicola De Zanche
Department of Medical Physics
Cross Cancer Institute
11560 University Avenue
Edmonton, Alberta, Canada
T6G 1Z2
Email: dezanche@ualberta.ca

ABSTRACT

This work describes the measurement of complex permittivity (or dielectric constant) of powders (water insoluble), solutions and suspensions using a parallel-plate capacitor cell. An impedance analyzer measures the cell's impedance at radio frequencies used in NMR and MRI (10–300 MHz) through an appropriate test fixture. The cell's impedance is fitted to an equivalent circuit using a MATLAB script or other software, and the permittivity of the material is extracted after calibration with known materials. The permittivity of the solid material is obtained from that of the powder suspension using known mixing rules. Measurements for most materials tested are in agreement with those obtained using standard coaxial probes. Some discrepancies are observed for loose powders because of the difficulty of controlling the amount of packing. For high-permittivity materials or conductive solutions an enhanced equivalent circuit has been found that characterizes the cell's behavior over the full frequency range.

INTRODUCTION

The measurement of the dielectric properties of materials is of significant importance in science and engineering, and numerous techniques have been developed to perform permittivity measurements over different ranges of frequencies (1), (2). In the transmission line method a sample of material is placed inside a section of a transmission line (waveguide or coaxial) and the permittivity (and permeability) are deduced from the transmission line's scattering (S) parameters. This is a broadband technique (1) but the mechanical construction of the transmission line is challenging. Similarly, a resonant cavity can also be used to measure permittivity by inserting a sample of the material and measuring the spectrum of resonances. While simpler in construction, it is a narrow band technique and is applicable only to low-loss materials. In the free-space method, electromagnetic waves are sent to a flat sample and the material's permittivity is deduced from the reflected signal. This technique requires a large, flat sample of material and is applicable at high frequencies (1 GHz or more) due to wavelength limits on minimum sample size (1), (3). Coaxial probe methods are those most commonly used at radio frequencies because only a contact with the material is required and they are applicable over a large frequency range (approximately 100 MHz to 100 GHz). However, coaxial probes lose accuracy at the lower end of the frequency range and can be used only for isotropic and homogeneous materials such as liquids, or solids with a flat surface. They are also not simple to make, while most commercial versions are aimed at higher frequencies and can only work with specific network analyzers.

This work describes the parallel-plate (capacitive) technique, which consists of sandwiching the sample between electrodes and measuring the impedance of the resulting capacitor (1). The method is simple, accurate, and is applicable at the relatively low frequencies encountered in MRI (well below 64 MHz to 400 MHz) (4). We apply the parallel-plate technique to ceramic powders and suspensions which can have relative permittivities of 100 or more. While coaxial probes are sensitive to local inhomogeneities in the material or occasional air bubbles, the parallel-plate cell is largely insensitive to these imperfections.

METHODS

Construction

The parallel-plate cell used in this work, shown in Figure 1, consists of two circular copper electrodes 30 mm in diameter, etched on FR4 circuit board and separated by a 6-mm-thick acrylic (PMMA) flange. One of the plates is glued to the flange and a connecting lead is soldered near the edge of each electrode to minimize connection lengths. A rubber O-ring provides a tight seal between the second plate and the flange when the six nylon screws are tightened to prevent leakage of liquids.

<**Figure 1**>

Theory

Equivalent circuits of the cell filled with a dielectric of unknown permittivity, including parasitics from the measurement setup, are shown in Figure 2, including the one proposed in Ref. (5) and a modified version.

<**Figure 2**>

Series or parallel resistances (R_s and R_p, respectively) and inductances (L_s and L_p) are mostly due to the test set up while R_d is dominated by the losses in the material under test (MUT). Total capacitance $C = C_0 + C_d$ is the combination of that of the empty cell (C_0) and MUT (C_d). The impedance of the circuits shown in Fig. 2 are given, respectively by

$$Z_{in}(\omega) = R_s + j\omega L_s + \frac{R_d}{1+j\omega C R_d}, \text{ and}$$

$$Z_{in}(\omega) = \frac{1}{\frac{1}{R_{P1}} + \frac{1}{j\omega L_P} + j\omega C_P} + \frac{R_d}{1 + j\omega C R_d} \quad (1)$$

Impedance measurements are performed at a number of frequencies and the circuit parameters are obtained by least-squares fitting to these equations in MATLAB (The Mathworks, Natick, MA) using the *fminsearch* function. Alternatively, the freely-available Zfit program (http://www.exality.com/blog/fitting-equivalent-

circuits-to-impedance-data/) provides the same functionality with a user-friendly interface and additional equivalent circuit models.

Calibration and Measurement

The relative permittivity and conductivity (in general, complex permittivity $\varepsilon = \varepsilon_r - i\varepsilon^{"}$) of the MUT are related to C_d and R_d , respectively, according to (1)

$$\varepsilon_r = C_d \left(\varepsilon_0 \frac{A}{d}\right)^{-1} = C_d K^{-1} \quad (2)$$

and

$$\sigma = \omega \cdot \varepsilon^{"} = \frac{1}{R_d}\left(\frac{d}{A}\right) = \frac{1}{K' \cdot R_d}. \quad (3)$$

Here K is the parallel-plate constant (in units of Farads) which depends on the cell's dimensions and $K' = \frac{K}{\varepsilon_0}$. All other circuit parameters are assumed to be constant. To find K and C_0 (stray capacitance due to edge fields through the PMMA flange), at least two materials with known dielectric properties are needed for calibration. In this work we chose air (empty cell, ε_r=1) and deionized water (ε_r=78.36 at 100 MHz and 25°C (6)) due to its availability and large permittivity. Introducing appropriate subscripts in Eq. 2 for the standard materials and rearranging we obtain

$$K = \frac{C_{Water} - C_{Air}}{\varepsilon_{Water} - \varepsilon_{Air}} \quad (4)$$

and

$$C_0 = C_{Air} - K \cdot \varepsilon_{r(air)}. \quad (5)$$

The cell's interior space is then filled with the material of interest (liquid, powder or suspension) and the cap is sealed by tightening the screws. Impedance of the cell is measured over the 10–300 MHz frequency range using the common Agilent 4396B combination analyzer in impedance analyzer mode through a 43961A

impedance test adapter and 16092A test fixture (Figure 3). Data are saved and exported for further processing on a PC as described in the Theory.

<**Figure 3**>

Materials

Measurements on powders, liquids and suspensions were performed, including 220-mesh alumina (Al_2O_3, Manus Abrasive Systems Inc.) and much finer $BaTiO_3$ (superscript A: Fisher Scientific, superscript B: Alfa Aesar, MA, USA). These ceramics in powder form have much lower bulk permittivity than the corresponding solid form due to presence of air between powder particles. Furthermore, the permittivity is strongly dependent on the grain size (7). To eliminate the effect of air between particles, the powder is mixed with varying amounts of demineralized water to achieve suspensions. Using Lichtenecker's logarithmic power law (8),

$$\varepsilon_r^{eff} = {\varepsilon_{rp}}^{f} \times \varepsilon_{rw}^{(1-f)}, \qquad 6$$

we can determine the permittivity of the solid ε_{rp} by knowing the volume fraction, f, the measured permittivity of the suspension ε_r^{eff}, and that of the liquid (water), ε_{rw}. The volume fraction is determined by measuring the masses of the two components and their respective densities.

Methanol, demineralized water and 4, 20, and 40 mM solutions of sodium chloride were also measured. However, there can be inaccurate permittivity measurements in such high-conductivity liquids due to electrolytic polarization that results from the ions in the dielectric-electrode boundary of the parallel-plate cell (2), (9), (10). Also, as conductivity of the material under test increases, the phase angle of the complex permittivity will be larger and the real part of the permittivity will be more difficult to resolve (11). To have detectable capacitance and avoid excessive stray fields, a small gap between plates is preferred but this enhances electrolytic polarization effects (5), (11).

Comparison to Coaxial Probes

The accuracy of the capacitive cell was evaluated by comparing the measurements to those obtained using coaxial probes from both Keysight (Santa Rosa, CA, USA) and Keycom (Tokyo, Japan). The Keysight 85070E Dielectric Probe Kit was connected to an Agilent E8362B network analyzer while the Keycom DPS16 (3.6 mm diameter) Open Mode Probe was connected to a Rohde and Schwarz ZVA67. The probes were immersed in the material taking care to avoid trapping air pockets or bubbles near the probe's sensitive volume (end of the coaxial line). This proved most challenging for the Keycom probe because its sensitive area is slightly recessed within the surrounding ground electrode.

RESULTS AND DISCUSSION

The measured and fitted impedance (resistance, R, and reactance, X) is shown in Figure **4** for some representative materials. As expected, the cell is capacitive over the chosen frequency range for materials with relatively low permittivity, while for higher permittivities the large capacitance and small inductance become resonant and the impedance is inductive at higher frequencies. In such cases fitting using the model of Figure **2a** must be confined to smaller frequencies in the capacitive region to avoid errors (Figure **4**c and d), or a modified circuit model such as that in Figure **2b** must be used. Calibration constants for the cell obtained from air and water measurements are K = 3.22 pF and C_0 = 2.29 pF. Complete complex permittivity results of the three measurement methods are listed in Table **1**.

<**Figure 4**>

For powders, the permittivity of the solid material is calculated from that of its suspension in water ($\varepsilon_{rw} = 78.5$) by knowing the volume fraction and applying Eq.5. (Table 2). The real part of the permittivity is compared graphically in Figure **5** and Figure **6**a, while Figure **6**b shows the loss tangent ($tan\,\delta = {\varepsilon^{"}}/{\varepsilon_r}$) of each material.

Agreement between the methods is excellent with the exception of powders and saline solutions. Discrepancies for $BaTiO_3$ powders are expected because of the difficulty of maintaining the same amount of packing among the three measurements, while those for saline solutions are due to electrolytic polarization as discussed in Materials. No systematic differences were found between the results from the dielectric cell and those from the coaxial probes. For powders and saline the differences between the two coaxial probes are of the same order as differences between the dielectric cell and the coaxial probes.

<Figure **5**>

<Figure **6**>

CONCLUSIONS

Measurement of the complex permittivity of powders and suspensions can be challenging with standard coaxial probes due to the common presence of inhomogeneities within the sample and air gaps between the probe and sample. The dielectric cell presented in this work is simple to fabricate and gives results that are comparable to those from coaxial probes over a wide range of materials. While coaxial probes lose accuracy at lower frequencies, the dielectric cell can be readily fabricated to operate at any frequency of interest in MRI and works with any impedance analyzer. The sensitive volume is larger than that of coaxial probes and therefore skewed results due to settling, bubbles or inhomogeneities are less likely. The dielectric cell is therefore well-suited for suspensions used for high-dielectric-constant pads.

Results show that measurements from different coaxial probes can differ as much as those between the dielectric cell and coaxial probes. Therefore we conclude that the accuracy of the dielectric cell method is comparable to that of coaxial probes. Electrolytic polarization effects in ionic liquids can be reduced or prevented by using platinum electrodes, by adding insulating layers, or by using a larger gap between the electrodes.

ACKNOWLEDGMENTS

We thank Mr. Ken Hennig for assistance with the construction of the cell and Keysight Technologies for access to the 85070E Dielectric Probe Kit. We gratefully acknowledge Dr. Rambabu Karumudi for providing the E8362B VNA, and Dr. Pedram Mousavi for access to the Keycom probe. We also thank Messrs. Daniel Oloumi and Adam Maunder for assistance with the coaxial probe measurements and Mr. Gerrit Barrere for writing, sharing, and providing support for the Zfit program.

References

1. Agilent Technologies: Basics of Measuring the Dielectric Properties of Materials. *Meas Tech* .

2. Kaatze U: Measuring the dielectric properties of materials. Ninety-year development from low-frequency techniques to broadband spectroscopy and high-frequency imaging. *Meas Sci Technol* 2013; 24:012005.

3. Kevin K.M. Chan, Adrian Eng-Choon Tan LL and KR: Material Characterization of Arbitrarily Shaped Dielectrics based on Reflected Pulse Characteristics. *IEEE Trans Microw Theory Tech* 2014.

4. Tereshchenko O V, Buesink FJK, Leferink FBJ: An overview of the techniques for measuring the dielectric properties of materials. In *Gen Assem Sci Symp URSI*. Istanbul; 2011:1–4.

5. Bottomley PA: A technique for the measurement of tissue impedance from 1 t o 100 MHz using a vector impedance meter. *J Phys E* 1978; 11:413–414.

6. Lide DR: "Permittivity (Dielectric constant) of water at various frequencies" in CRC Handbook of Chemistry and Physics. *CRC Press Boca Raton, FL* :3485.

7. Webb AG: Dielectric Materials in Magnetic Resonance. *Concepts inMagnetic Reson Part A* 2011; 38A(4):148–184.

8. Sihvola A: Mixing rules with complex dielectric coefficients. *Subsurf Sens Technol Appl* 2000; 1:393–415.

9. Gough SR: A Low Temperature Dielectric Cell and the Permittivity of Hexagonal Ice to 2 K. *Can J Chem* 1972; 50:3046–3051.

10. Mazzeo B a, Chandra S, Mellor BL, Arellano J: Temperature-stable parallel-plate dielectric cell for broadband liquid impedance measurements. *Rev Sci Instrum* 2010; 81:125103.

11. Grove TT, Masters MF, Miers RE: Determining dielectric constants using a parallel plate capacitor. *Am J Phys* 2005; 73:52.

Figure Captions

Figure 1: Parallel plate cell: (a) drawing and dimensions, (b) fabricated prototype. (*color online only*)

Figure 2: Equivalent circuits for the capacitive measurement cell. a) standard circuit used in Ref. (5) and b) modified circuit that improves fits in high-loss or high-permittivity materials.

Figure 3: Impedance measurement setup, including Agilent 4396B combination analyzer, 43961A impedance test adapter and 16092A test fixture. (*color online only*)

Figure 4: Resistance and reactance measured (gray) and fitted (black) for some representative samples (a) $BaTiO_3^A$ powder, (b) methanol, (c) 4 mM saline, (d) f=0.353 $BaTiO_3^B$ suspension. Fitting results for the model of **Figure 2a** are shown within rectangles and the corresponding frequency range is indicated by the support of the solid black lines. Improved fitting results for (c) and (d) are obtained using the model of **Figure 2b (**black dash-dot lines).

Figure 5: Comparison between cell (model in **Figure 2a**) and coaxial probe measurements of real permittivity ($\boldsymbol{\varepsilon_r}$) at 100 MHz. Agreement is excellent with the exception of powders and saline solutions (horizontal and vertical ellipses, respectively). (*color online only*)

Figure 6: Comparison of (a) real permittivity and (b) loss tangent ($\mathbf{tan}\,\boldsymbol{\delta}$) for each material at 100 MHz. Dielectric cell measurements use the model in **Figure 2a.** Largest differences are highlighted in rectangles. (*color online only*)

Tables

Table 1: Complex permittivity measured using the dielectric cell (model in **Figure 2a**) and coaxial probes at 100 MHz.

Material	Agilent probe ε	Keycom probe ε	Dielectric Cell ε
$BaTiO_3^A$ powder	3.66+j0.07	2.50-j0.09	6.14+j0.15
$BaTiO_3^B$ powder	3.36+j0.08	13.8-j0.93	8.97+j0.15
Al_2O_3 powder	3.03+j0.04	2.82+j0.15	2.64+j0.087
Demineralized water	78.4-j0.75	80.1-j0.51	78.5-j1.45
Methanol	33.5-j1.92	33.6-j1.98	31.5-j1.04
Saline 4 mM	77.4-j40.5	78.9-j40.2	72.3-j10.0
Saline 20 mM	74.3-j316	74.9-j319	103-j589
Saline 40 mM	73.2-j541	75.9-j574	177-j1619
f=0.5 alumina suspension	41. 8-j5.82	41.1-j3.64	33.5-j3.23
f=0.53 alumina suspension	37.1-j4.16	26.8-j2.44	26.5-j1.85
f=0.353 $BaTiO_3^A$ suspension	284-j184	221-j89.6	261-j15.6
f=0.42 $BaTiO_3^A$ suspension	327-j206	216-j78.6	280-j17.0
f=0.353 $BaTiO_3^B$ suspension	271-j29.1	228-j17.4	265-j19.6
f=0.246 $BaTiO_3^B$ suspension	120-j30.5	179-j13.3	177-j14.4

Table 2: Volume fractions and permittivity (real part) of the dry powders (see **Materials**).

	Al_2O_3	**$BaTiO_3^A$**	**$BaTiO_3^B$**
Mass density (g/mL)	Appx. 4.0	6.08	5.85
Volume fraction ($f=V_{powder}/V_{total}$)	0.5	0.35	0.35
Calculated ε_r of the solid material	14.25	2360.3	2464.6

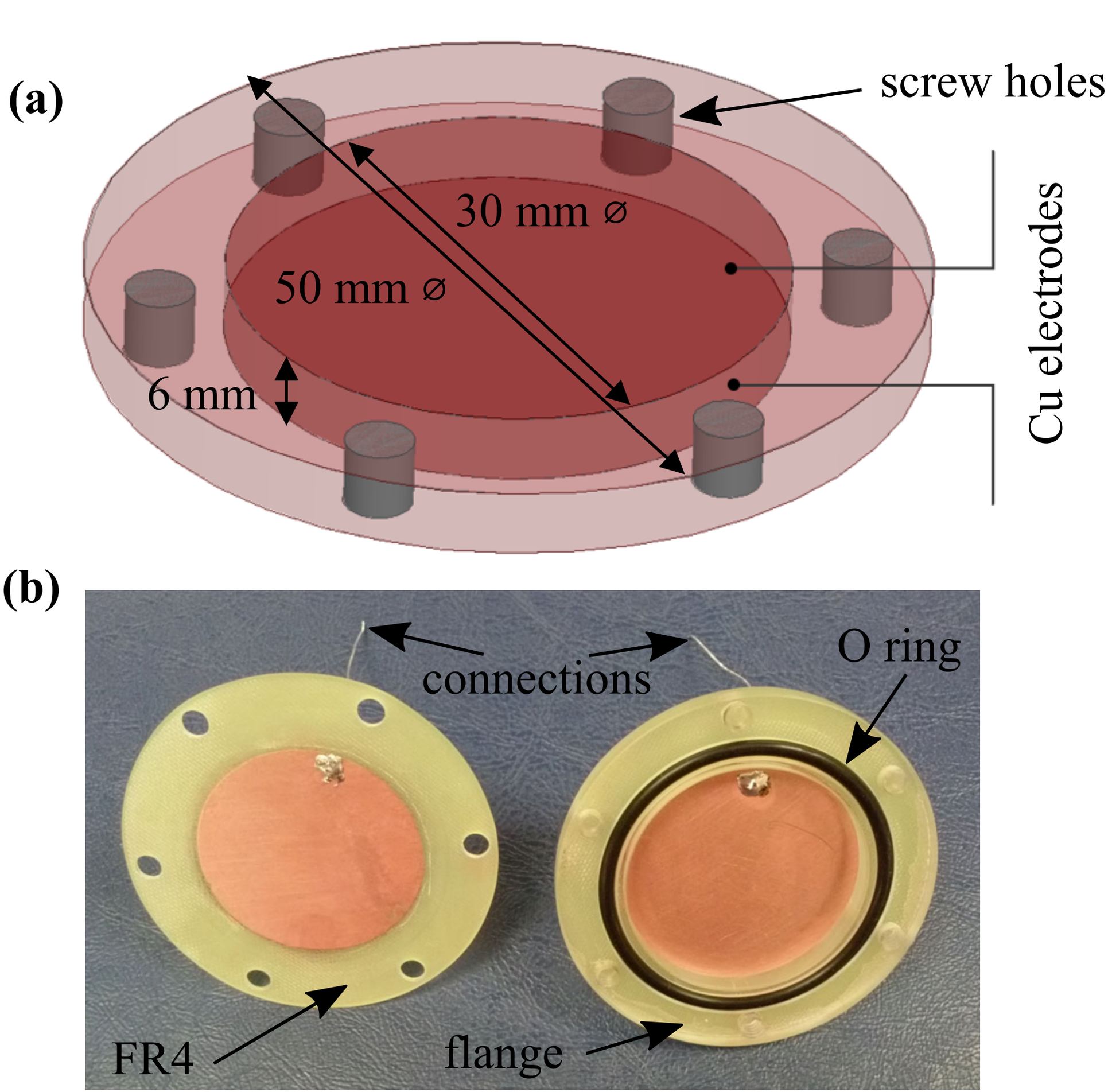
(a)
screw holes
30 mm ⌀
50 mm ⌀
6 mm
Cu electrodes
(b)
connections
O ring
FR4
flange

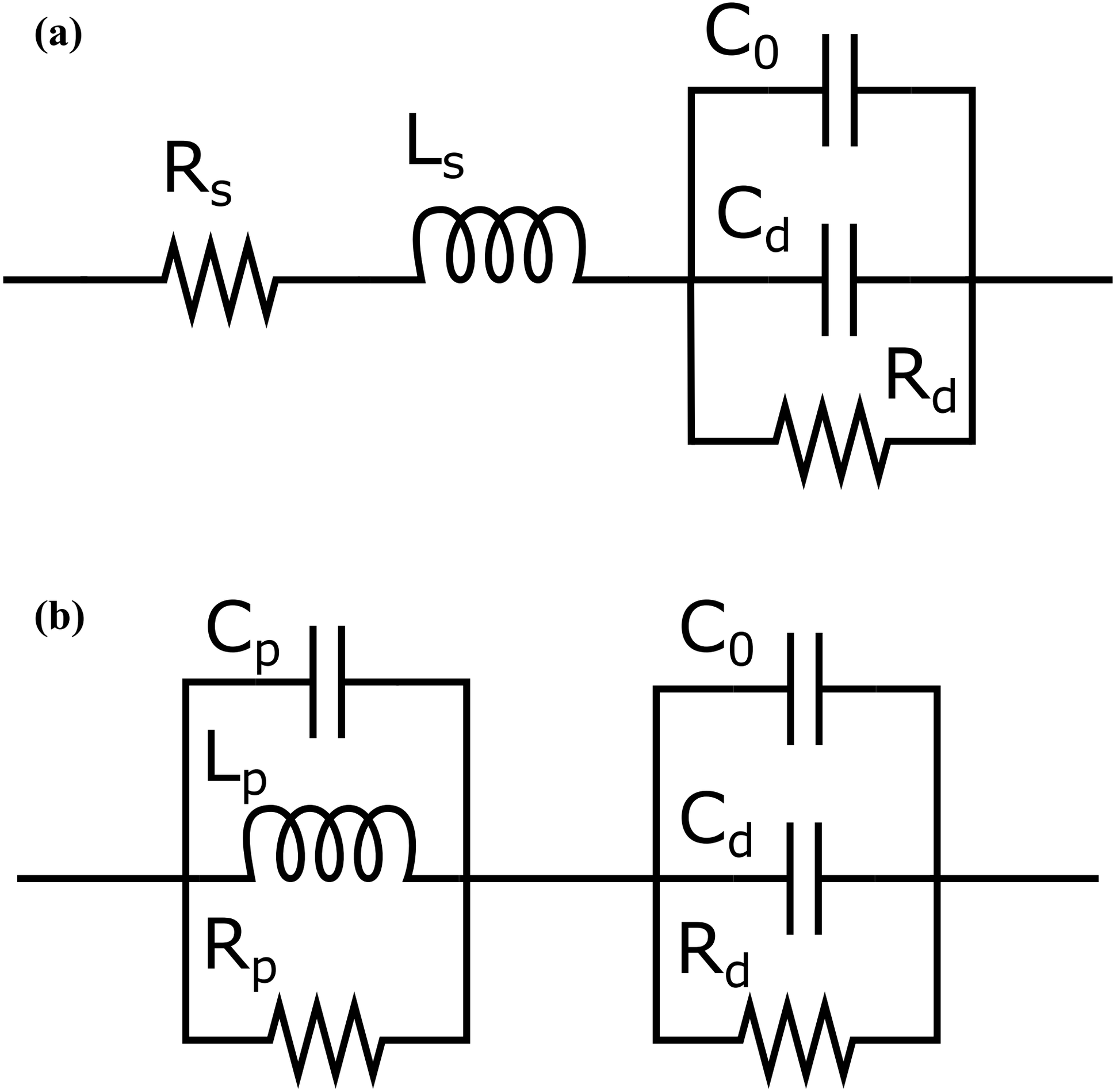
(a)
C_0
L_s
R_s
C_d
R_d
(b)
C_p
C_0
L_p
C_d
R_p
R_d

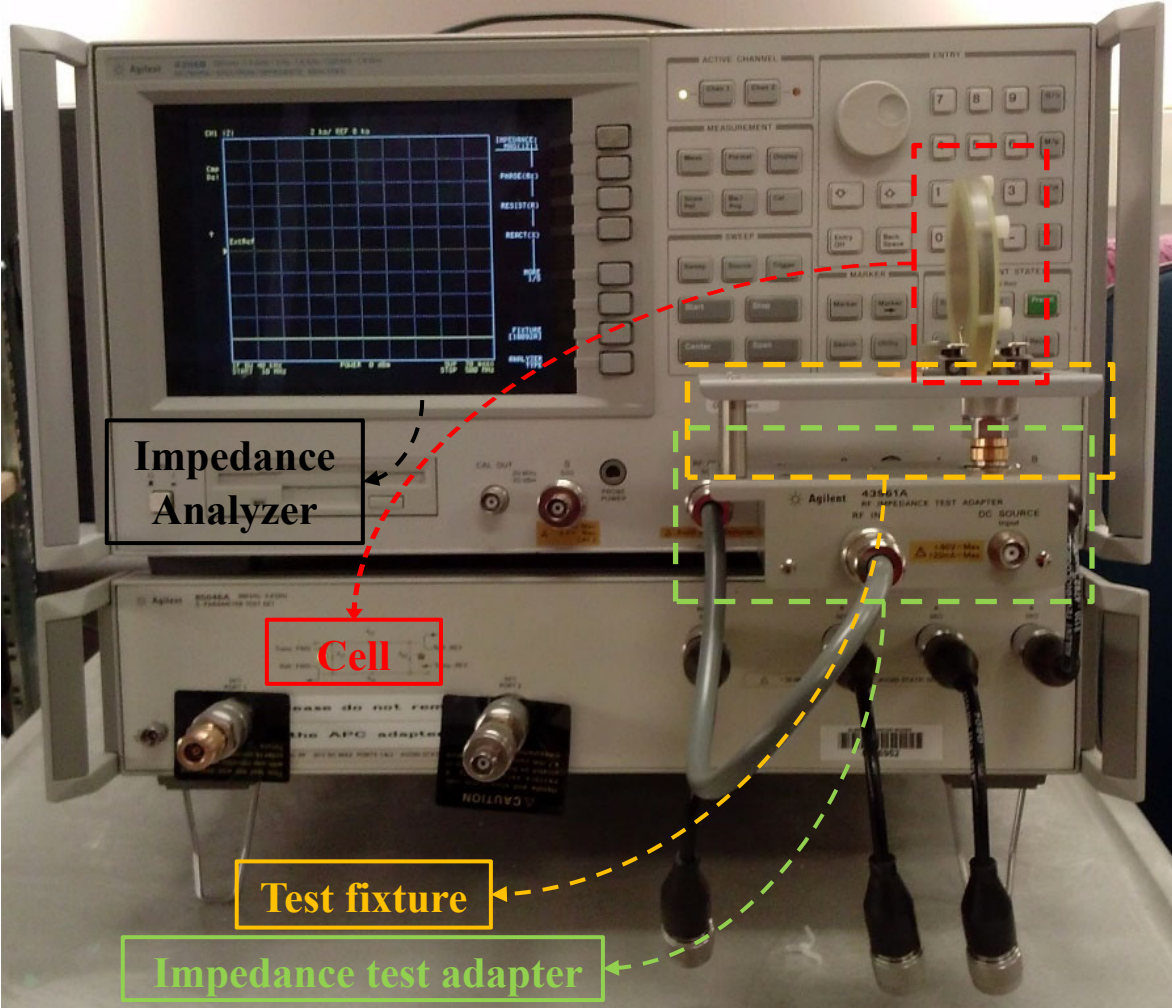
Impedance Analyzer
Cell
Test fixture
Impedance test adapter

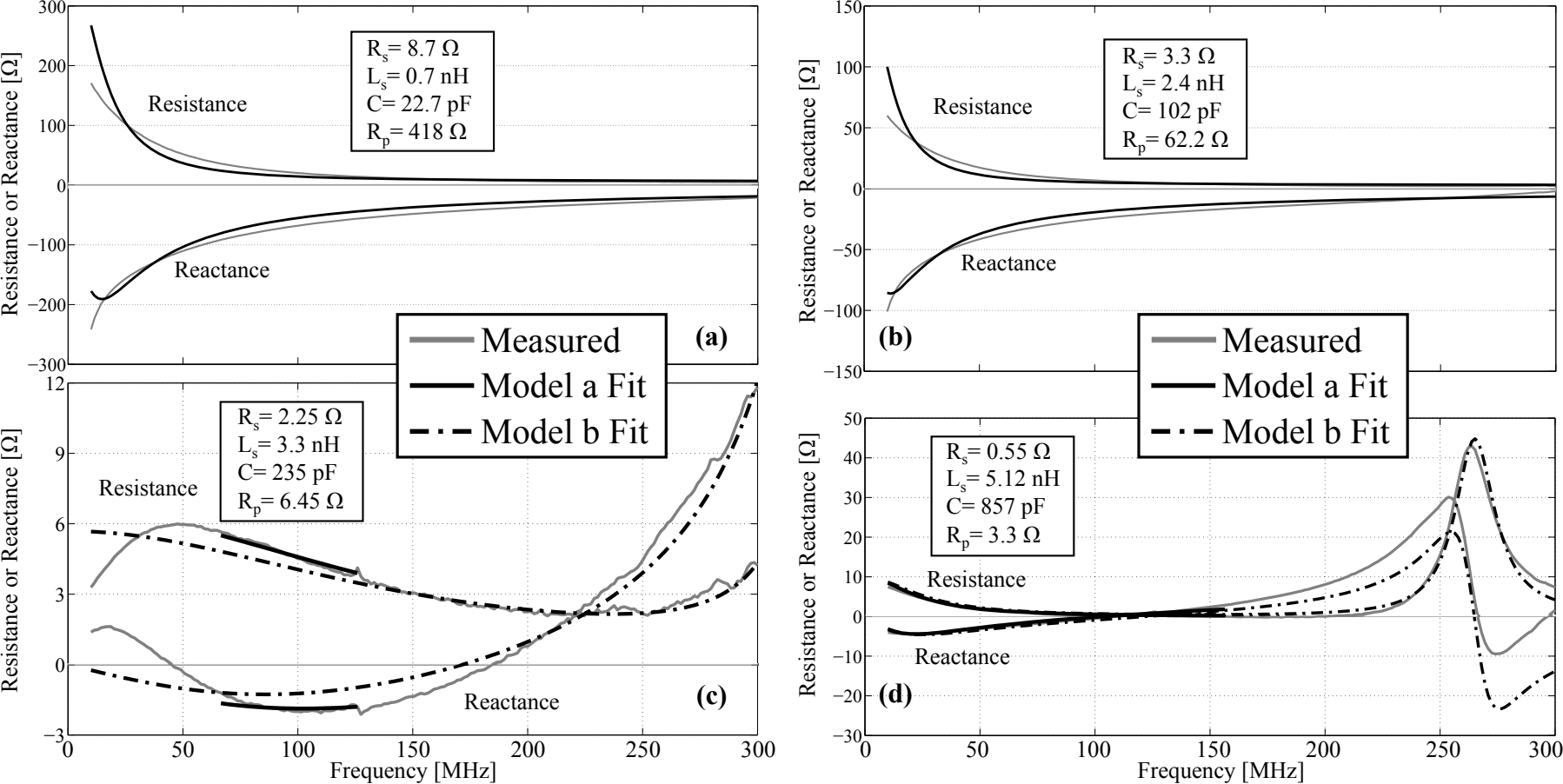
Resistance or Reactance [Ω]
Frequency [MHz]
Resistance
Reactance
Measured
Model a Fit
Model b Fit
(a)
R_s= 8.7 Ω
L_s= 0.7 nH
C= 22.7 pF
R_p= 418 Ω
(b)
R_s= 3.3 Ω
L_s= 2.4 nH
C= 102 pF
R_p= 62.2 Ω
(c)
R_s= 2.25 Ω
L_s= 3.3 nH
C= 235 pF
R_p= 6.45 Ω
(d)
R_s= 0.55 Ω
L_s= 5.12 nH
C= 857 pF
R_p= 3.3 Ω

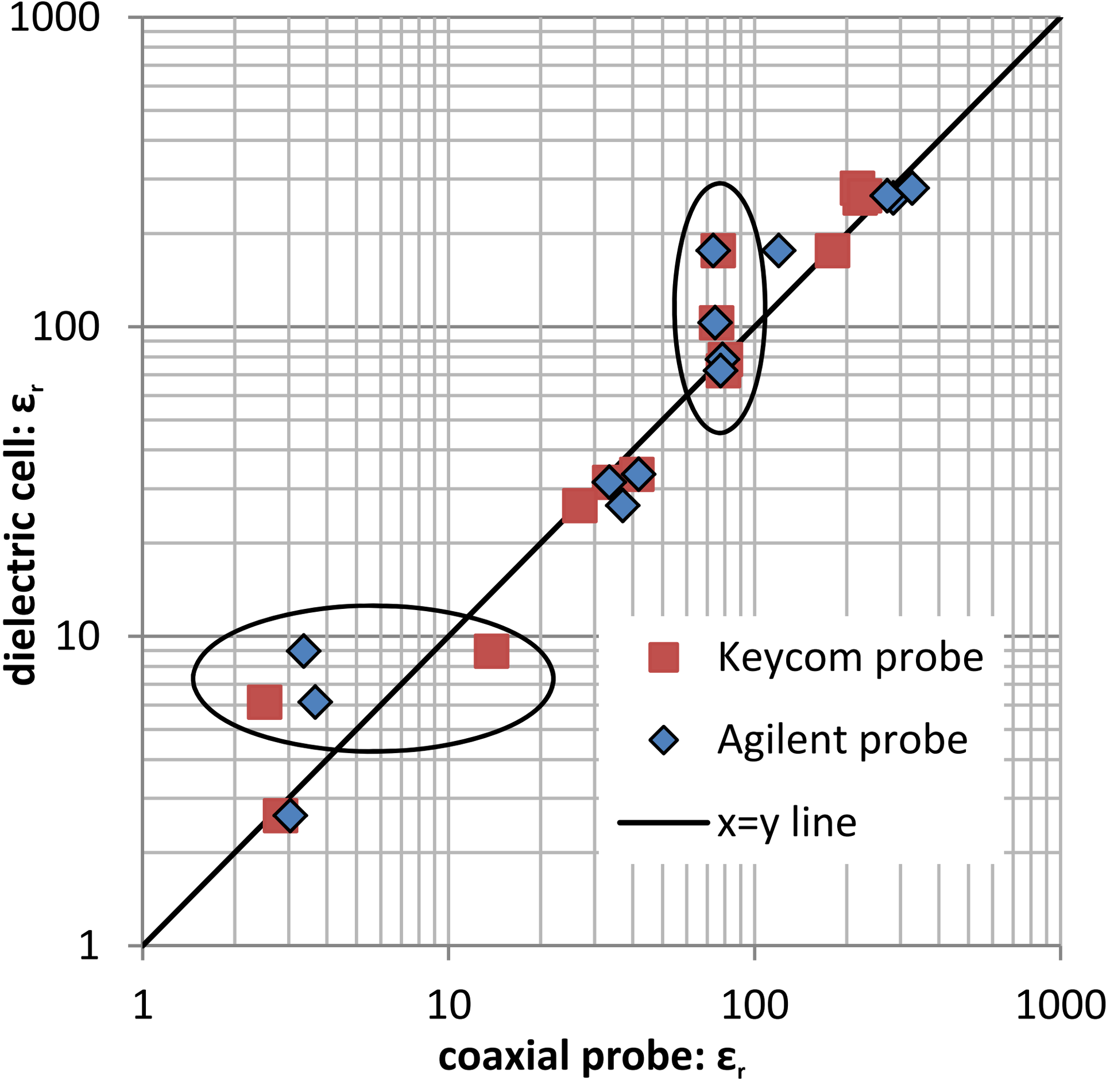
1000
100
10
1
dielectric cell: εr
1
10
100
1000
coaxial probe: εr
Keycom probe
Agilent probe
x=y line

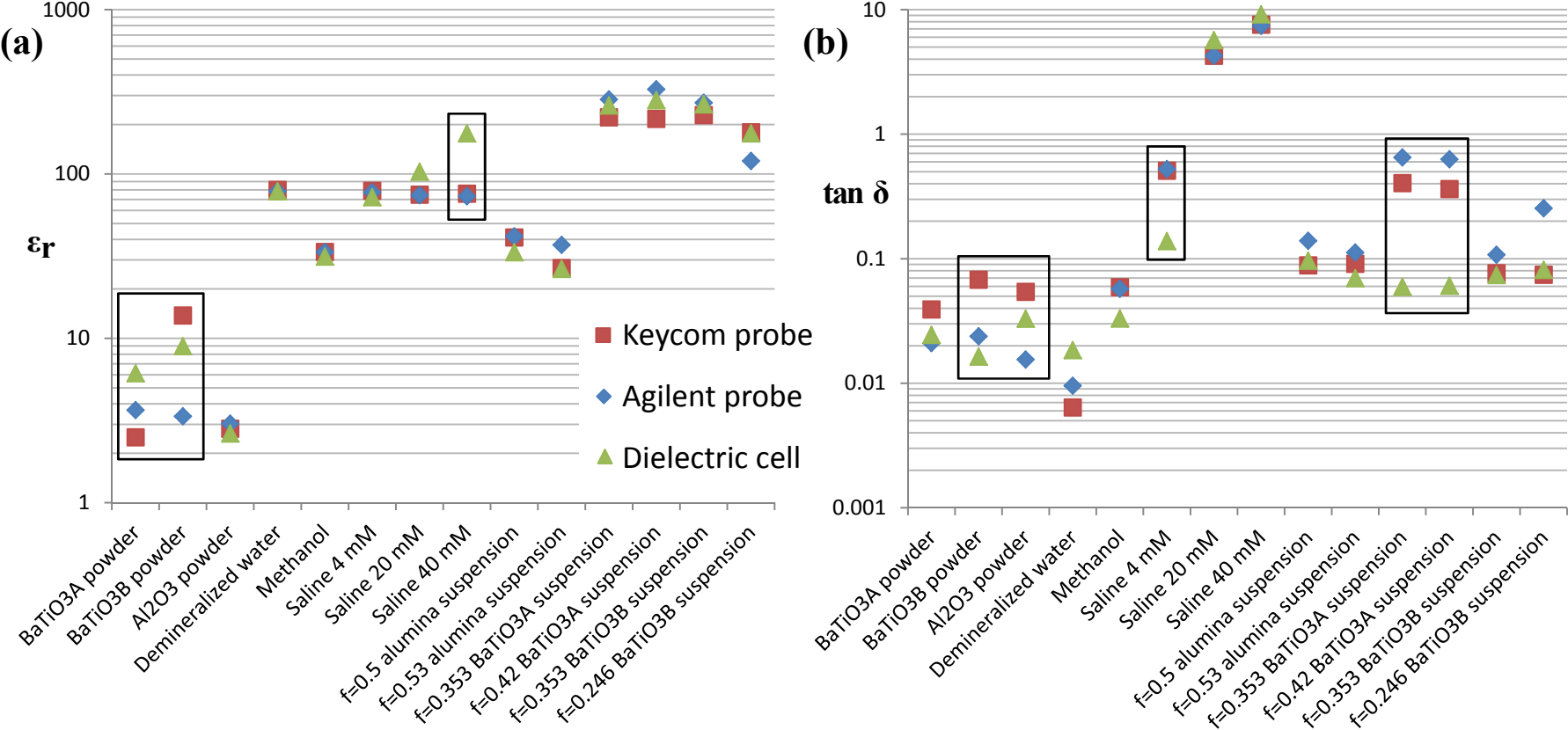
(a)
1000
100
10
1
εr
Keycom probe
Agilent probe
Dielectric cell
BaTiO3A powder
BaTiO3B powder
Al2O3 powder
Demineralized water
Methanol
Saline 4 mM
Saline 20 mM
Saline 40 mM
f=0.5 alumina suspension
f=0.53 alumina suspension
f=0.353 BaTiO3A suspension
f=0.42 BaTiO3A suspension
f=0.353 BaTiO3B suspension
f=0.246 BaTiO3B suspension
(b)
10
1
0.1
0.01
0.001
tan δ
BaTiO3A powder
BaTiO3B powder
Al2O3 powder
Demineralized water
Methanol
Saline 4 mM
Saline 20 mM
Saline 40 mM
f=0.5 alumina suspension
f=0.53 alumina suspension
f=0.353 BaTiO3A suspension
f=0.42 BaTiO3A suspension
f=0.353 BaTiO3B suspension
f=0.246 BaTiO3B suspension